

BCR ligation selectively inhibits IgE class switch recombination

Adam K. Wade-Vallance^{1,2,3,5}, Zhiyong Yang^{2,3}, Jeremy B. Libang^{1,2,3,*}, Ananya R. Krishnapura^{1,2,3,*}, James B. Jung^{2,3,6,*}, Emily W. Matcham^{2,3,7}, Marcus J. Robinson^{2,3,8}, and Christopher D. C. Allen^{2,3,4,#}

¹Biomedical Sciences Graduate Program, ²Cardiovascular Research Institute, ³Sandler Asthma Basic Research Center, and ⁴Department of Anatomy, University of California, San Francisco, CA 94143, USA

⁵Present address: Lymphocyte Biology Section, Laboratory of Immune System Biology, National Institute of Allergy and Infectious Diseases, National Institutes of Health, Bethesda, MD 20892, USA

⁶Present address: Gilead Sciences Inc., Foster City, CA 94404, USA

⁷Present address: CRUK Cambridge Institute, University of Cambridge, Cambridge CB2 0RE, UK

⁸Present address: Department of Immunology, Monash University, Melbourne, VIC 3004, Australia

*Equal contributions

#Correspondence should be addressed to:

Christopher D. C. Allen, Ph.D.

Address: UCSF
CVRI, Box 3122
555 Mission Bay Blvd S
San Francisco, CA 94143

Email: Chris.Allen@ucsf.edu

Phone: 415-476-5178

Abstract

Mechanisms that restrict class switch recombination (CSR) to IgE limit the subsequent production of IgE antibodies and therefore the development of allergic disease. Mice with impaired B cell receptor (BCR) signaling have significantly increased IgE responses, consistent with a role for BCR signaling in IgE regulation. While prior work focused on BCR signaling in IgE-expressing cells to explain these findings, it has been reported that BCR signaling can reduce CSR. Therefore, we investigated the possibility that IgE CSR might be particularly sensitive to inhibition by BCR signaling in unswitched B cells. We found that immunization of mice with high-affinity antigen resulted in reduced representation of IgE-expressing cells among germinal center B cells and plasma cells relative to a low-affinity antigen. Mechanistic experiments with cultured mouse B cells demonstrated that BCR ligands selectively inhibited IgE CSR in a dose-, affinity-, and avidity-dependent manner. Signaling via Syk was required for the inhibition of IgE CSR following BCR stimulation, whereas inhibition of the PI3K subunit p110 δ increased IgE CSR independently of BCR ligation. The inhibition of IgE CSR by BCR ligands synergized with IL-21 or TGF β 1. BCR ligation also inhibited CSR to IgE in human tonsillar B cells, and this inhibition was also synergistic with IL-21. These findings establish that IgE CSR is uniquely susceptible to inhibition by BCR signaling in mouse and human B cells, with important implications for the regulation and pathogenesis of allergic disease.

1 Introduction

2 Type-1 hypersensitivity responses in allergic disease result from the production of IgE antibodies
3 specific for food and environmental antigens. Prior to IgE production, B cells must first undergo
4 IgE class switch recombination (CSR). Whereas IgE CSR can be readily induced by stimulating
5 B cells in cell culture, the abundance of IgE in serum is orders of magnitude less than that of IgG.
6 The scarcity of IgE *in vivo* implies the existence of regulatory mechanisms absent from typical *in*
7 *vitro* systems.¹ For example, our prior work identified IL-21 as a major negative regulator of IgE
8 CSR.² An additional potential source of regulation is cognate antigen. Indeed, when cognate
9 antigen directly ligates B cell receptors (BCRs) on IgE plasma cells (PCs; used to collectively refer
10 to both plasma cells and plasmablasts), this results in their elimination.³ Stimulation of the BCR
11 can also broadly inhibit class-switching,⁴⁻⁷ and prior studies from our lab and others found
12 selectively increased IgE responses in mice with impaired BCR signaling.⁸⁻¹⁰ However, evidence
13 for whether BCR stimulation might selectively affect IgE CSR is mixed.^{6,11}

14
15 B cell antigen encounter initiates a complex array of BCR signaling pathways that coordinate a
16 variety of cellular responses. The incipient events of BCR signaling include the formation of the
17 “BCR signalosome” through a series of interactions between Syk, BLNK, Btk, and PLC γ 2, among
18 others.¹² This process is reinforced through the activation of PI3K (composed of p110 catalytic
19 and p85 regulatory subunits) to produce phospholipids that recruit several BCR signalosome
20 components and other molecules to the plasma membrane.¹² Mice with disrupted p110 δ (the most
21 abundant p110 isoform in B cells)¹³⁻¹⁵ signaling produce exaggerated IgE responses to type-2
22 immunizations.^{8,10,16} These observations may relate to effects on IgE CSR, as CSR is broadly
23 inhibited in mice with enhanced PI3K activity, and treating mice or cells with PI3K inhibitors
24 increases IgE.^{4,16-20} Increased IgE responses have also been reported in mice with heterozygous
25 mutations in *Syk*, homozygous mutations in *Blnk*, or upon pharmacologic inhibition of Btk.¹⁰ Syk,
26 BLNK, and Btk are known to be important in cells that have already undergone IgE CSR due to
27 their roles in antigen-independent signaling of the IgE BCR^{8,10} and in BCR ligation-induced IgE
28 PC apoptosis.³ It is unclear if these molecules also play a role in the inhibition of IgE CSR
29 downstream of BCR stimulation.

30
31 Here, we investigated the role of BCR signaling in IgE CSR. We first used genetic and comparative
32 immunization-based strategies in mice to demonstrate that stronger BCR:antigen interactions
33 resulted in reduced representation of IgE cells in the GC and among extrafollicular PCs. BCR
34 stimulation inhibited IgE CSR to a greater extent than IgG1 CSR, and CSR inhibition was dose-,
35 affinity-, and avidity-dependent. We identified a selective effect of BCR stimulation on ϵ germline
36 transcripts, implicating a transcriptional mechanism for IgE CSR inhibition. At the level of
37 signaling molecules, Syk was required, and PKC signaling was sufficient, for the selective
38 inhibition of IgE CSR following BCR stimulation. Interestingly, p110 δ was not required and
39 instead suppressed IgE CSR independently of BCR stimulation. We found synergistic inhibition
40 of IgE CSR with BCR stimulation and either IL-21 or TGF β 1. BCR stimulation also selectively
41 inhibited IgE CSR in human B cells, which was also synergistic with IL-21.

42 **Results**

43 **BCR stimulation strength inversely correlates with IgE-switched cells**

44 To query how BCR:antigen binding strength might selectively regulate IgE CSR *in vivo*, we
45 performed adoptive transfers of Hy10 B cells whose BCRs are specific for avian egg lysozyme.
46 Congenic recipient mice were then immunized with antigen of low or high affinity for the Hy10
47 BCR (duck egg lysozyme [DEL] or hen egg lysozyme [HEL], respectively).²¹ One week later, IgE,
48 but not IgG1, cells were less frequent among both GC B cells and PCs in the draining lymph nodes
49 (dLNs) of recipients immunized with HEL compared to DEL (Figure 1A). These data provide
50 evidence for a selective, inhibitory effect of antigen affinity on the frequency of IgE-expressing
51 cells *in vivo*.

52
53 We next sought to determine if modulating BCR signaling strength through the surface expression
54 level of the BCR would impact IgE switching. Ig α (aka CD79a / Mb1) is one of two obligate
55 ITAM-containing protein components of the BCR, and is also critical for BCR surface
56 expression.^{10,22} We therefore reasoned that Ig α -heterozygous mice might have reduced surface
57 BCR expression. Indeed, Ig α ^{+/-} naïve follicular B cells had reduced surface IgM and IgD relative
58 to WT cells (Figure 1B). Following immunization, Ig α ^{+/-} mice had increased frequencies of IgE
59 cells within both the GC and PC compartments (Figure 1C). Interestingly, these mice also had a
60 subtle increase in IgG1 GC B cells and decrease in IgG1 PCs, consistent with previously described
61 roles for BCR signaling in PC differentiation.^{23,24} Overall, these data expand upon prior findings
62 that weakened BCR signaling results in greater IgE responses^{8,10} and are consistent with the
63 hypothesis that IgE CSR is especially susceptible to inhibition by BCR ligation.

64
65 To dissect the effect of BCR ligation on IgE CSR we induced B cells, purified from murine
66 splenocytes, to undergo CSR in cell culture using IL-4 and α CD40. BCR stimulation with an anti-
67 BCR antibody (goat anti-mouse IgD [α IgD]), but not control antibody (goat gamma globulin
68 [GGG]), resulted in a greatly reduced frequency of IgE cells in the culture (~4.3-fold), with a lesser
69 reduction in IgG1 cells (~1.2-fold, Figure S1A-B). As we observed an overall reduction in class-
70 switching after BCR stimulation (Figure S1C-D), we examined the frequency of IgE cells among
71 class-switched cells and found that BCR stimulation resulted in greatly reduced representation of
72 IgE cells within the class-switched compartment, while the representation of IgG1 cells was
73 increased (Figure S1E-F). These data suggest that BCR stimulation has a selective negative impact
74 on IgE CSR.

75
76 We next asked whether these findings were generalizable to different anti-BCR antibodies as well
77 as cognate antigen. While α IgD treatment resulted in the greatest dose-dependent reduction in IgE
78 of anti-BCR antibodies we measured, both goat anti-mouse IgM (α IgM) and goat anti-mouse Ig
79 kappa light chain (α Ig κ) produced significant reductions in IgE (Figure 1D-E). To investigate the
80 impact of cognate antigen on IgE CSR, we purified and cultured Ig λ light chain-expressing cells
81 from B1-8i mice.²⁵ B1-8i mice have a pre-arranged heavy chain VDJ that endows most B cells
82 expressing λ light chains with binding specificity towards the hapten 4-hydroxy-3-nitrophenyl
83 (NP) and with 20-fold higher binding strength towards the hapten 4-hydroxy-3-iodo-5-nitrophenyl
84 (NIP).²⁶ We assessed the impact of cognate antigen dose, affinity, and avidity on IgE and IgG1
85 CSR by treatment with different doses of high-valency, higher-affinity antigen (NIP₂₄BSA); high-
86 valency, lower-affinity antigen (NP₂₅BSA); or low-valency, lower-affinity antigen (NP₄BSA). As
87 we previously found that cognate antigen could eliminate IgE PCs,³ we focused our present

88 investigation on B cells by including antigen from the beginning of cell culture, using substantially
89 lower doses, and performing our analysis prior to the bulk of PC differentiation. We found that all
90 three cognate antigens resulted in dose-dependent reductions in the representation of IgE-
91 expressing cells (Figure 2A), although the potency of the different cognate antigens varied over
92 orders of magnitude according to their affinity and valency. Notably, the representation of IgE
93 cells in culture was more sensitive to inhibition by cognate antigen than IgG1, as revealed by
94 intermediate doses of all three cognate antigens which reduced the representation of IgE but not
95 IgG1 cells. Examining the representation of IgE- and IgG1-switched cells among class-switched
96 (IgM⁻IgD⁻) cells revealed that, even with powerful BCR ligation, the representation of IgE cells
97 was reduced more greatly relative to other class-switched cells, whereas the representation of IgG1
98 cells was maintained or increased (Figure 2B). To quantitate the relative effects of cognate antigen
99 on IgE and IgG1 CSR, we performed a normalized analysis (Figure 2C). This analysis confirmed
100 that for each cognate antigen there were intermediate doses which led to decreases in IgE cells,
101 but not IgG1 cells. While we observed reductions in IgG1 cells at high doses of antigen, these
102 doses also resulted in greater reductions in IgE cells. Overall, these data support that ligating BCRs
103 on B cells preferentially reduces IgE CSR.

104

105 **BCR stimulation inhibits IgE CSR by downmodulating ϵ germline transcription**

106 We considered multiple possibilities by which stimulating the BCR could lead to reduced numbers
107 of IgE cells. As class-switching is linked to cell division, and IgE requires more cell divisions to
108 emerge relative to IgG1,²⁷ one possibility is that BCR signaling limits the opportunity for IgE CSR
109 to occur by reducing proliferation. To distinguish potential effects on proliferation versus CSR we
110 loaded B cells with CellTrace Violet (CTV) and examined at each division number whether BCR
111 stimulation affected the fraction of IgE or IgG1 cells. CTV fluorescence is reduced 2-fold with
112 each cell division, and after four days of culture, we were able to visualize seven distinct
113 populations of B cells based on the intensity of their CTV staining (Figure 3A). Whereas IgG1
114 cells were first detectable after 3 divisions, IgE cells remained absent until 5 divisions, consistent
115 with prior work (Figure 3B-C).²⁷ Relative to control treatment, BCR stimulation resulted in a
116 reduction in the fraction of cells switched to IgE across all cell divisions at which they were present
117 (Figure 3B). This finding suggests that BCR stimulation reduces IgE CSR directly rather than as
118 a secondary outcome of impaired proliferation. Meanwhile, BCR stimulation resulted in a mild
119 reduction in the fraction of IgG1-switched cells at divisions 2 through 5, but IgG1 CSR normalized
120 and trended towards being increased at divisions 6+ (Figure 3C-D). These results suggest that
121 whereas BCR stimulation merely delays IgG1 CSR to later cell divisions, it directly inhibits IgE
122 CSR.

123

124 To gain further insight in the mechanism of IgE CSR inhibition, we quantified ϵ and γ_1 germline
125 and post-switch transcripts (GLT and PST, respectively) as well as *Aicda* transcripts (encoding
126 AID) and compared them between BCR-stimulated and control B cell cultures. GLTs are
127 transcribed from the I (e.g. I $_{\epsilon}$ or I $_{\gamma_1}$) region upstream of the switch region for all class-switched
128 antibody isotypes and their production is a pre-requisite for a B cell to undergo CSR to that isotype.
129 It is thought that this is due to their importance in ‘opening up’ local chromatin.^{28,29} The completion
130 of CSR can be detected by the expression of PSTs, which are transcribed from I $_{\mu}$ through the
131 recombined switch regions and the downstream constant region. BCR stimulation resulted in a
132 significant >50% reduction in ϵ GLT at D2. In contrast, we observed no significant difference in
133 γ_1 GLT, with a trend toward an increase (28%). In addition, at D3, BCR stimulation led to a strong

134 (64%) reduction in ϵ PST with a subtle (13%) impact on γ_1 PST (Figure 3D). *Aicda* transcripts were
135 equivalent at D2, but at D3 there was a minor (15%) reduction in the α IgD condition. Overall, the
136 more substantial reduction in ϵ PST than γ_1 PST was consistent with the greater impact of BCR
137 ligation on numbers of IgE-switched versus IgG1-switched cells observed above by flow
138 cytometry. Furthermore, the PST data came from D3 of culture, prior to the emergence of most
139 membrane IgE-positive cells, reinforcing our observation in the above CTV experiments that CSR
140 to IgE was reduced at the earliest points at which it could be observed. The reduction in ϵ GLT, but
141 not γ_1 GLT, at D2 is consistent with the notion that the effect of BCR ligation on IgE CSR occurs
142 via altered transcription at the epsilon locus, rather than through changes in *Aicda* transcripts,
143 which we found were unchanged at D2 or reduced only subtly at D3.

144

145 **IgE CSR inhibition by BCR stimulation is principally mediated by Syk**

146 As discussed earlier, substantial prior literature has focused on the role of PI3K signaling in
147 CSR.^{4,7,16,17,19,20} Therefore, we set out to resolve whether PI3K δ , the main PI3K isoform expressed
148 in B cells, is necessary for the inhibition of IgE CSR by BCR stimulation. Consistent with prior
149 work, treatment with the PI3K δ inhibitor nemiralisib resulted in dose-dependent increases in IgE
150 in the absence of BCR ligation (Figure 4A). However, regardless of the dose of inhibitor, IgE CSR
151 remained strongly susceptible to inhibition by BCR stimulation (Figure 4A). To precisely
152 determine whether PI3K δ signaling is required for IgE CSR inhibition by BCR stimulation, we
153 performed a normalized analysis. This analysis revealed that the addition of α IgD reduced IgE by
154 ~70% regardless of the presence of PI3K δ inhibitor or vehicle control (Figure 4B). These results
155 confirmed that PI3K δ regulates IgE,^{16,20} but was not required for the inhibition of IgE CSR by
156 BCR stimulation.

157

158 We considered various possibilities to explain this result. It could be that an isoform of p110 other
159 than p110 δ (e.g. p110 α) was responsible for inhibiting IgE CSR downstream of BCR stimulation.
160 Alternatively, there might be redundancy between p110 isoforms, meaning that a complete
161 blockade was required to rescue IgE CSR from inhibition by BCR stimulation. Another possibility
162 is that a non-PI3K-mediated pathway downstream of BCR signaling is responsible for inhibiting
163 IgE CSR. To test these possibilities, we performed further experiments with different inhibitors.
164 To assess if a more complete blockade of p110 signaling could interfere with the inhibition of IgE
165 CSR by BCR stimulation, we selected a second p110 δ inhibitor (idelalisib) to validate our earlier
166 findings as well as two pan-p110 inhibitors (omipalisib and wortmannin), one of which also
167 inhibits mTOR (mammalian target of rapamycin; omipalisib). We also tested inhibitors of Syk
168 (PRT062607) and Btk (ibrutinib) to assess an alternative pathway by which BCR stimulation might
169 inhibit IgE CSR. Strikingly, Btk and Syk inhibitors both dose-dependently rescued IgE CSR in the
170 presence of α IgD, but, in the absence of α IgD, left IgE CSR mostly unaffected (Figure 4C).
171 Meanwhile, both idelalisib and omipalisib increased IgE CSR regardless of the presence or
172 absence of α IgD (Figure 4C, see Supplementary Table 1 for statistical comparisons), similar to our
173 earlier results with the PI3K δ inhibitor. Surprisingly, wortmannin did not increase IgE CSR in the
174 absence of BCR stimulation, unlike the other p110 inhibitors tested. We confirmed the activity of
175 our wortmannin at the relevant dose by verifying its ability to block BCR ligation-dependent S6
176 phosphorylation (Figure S2). While idelalisib and omipalisib treatment increased IgE CSR, we
177 still observed decreases in IgE CSR following α IgD treatment. To further evaluate if the effects of
178 the p110 inhibitors were independent of BCR stimulation, we again performed a normalized
179 analysis. This analysis confirmed that the highest dose of Syk inhibitor resulted in a complete

180 rescue of IgE CSR from inhibition by BCR stimulation, while maximal Btk inhibition resulted in
181 a substantial yet incomplete rescue (Figure 4D). The p110 δ inhibitor idelalisib achieved no
182 significant rescue of IgE CSR inhibition by BCR stimulation, confirming our earlier result. The
183 pan-p110 inhibitor wortmannin also did not rescue IgE CSR, whereas the pan-p110 + mTOR
184 inhibitor omipalisib achieved a moderate rescue. This finding could suggest a contribution of
185 mTOR to IgE CSR inhibition by BCR stimulation. Taken together, these data indicate that PI3K
186 signaling is not required for IgE CSR inhibition by BCR stimulation. Meanwhile, signaling
187 through Syk, with a prominent role for Btk, is required for the inhibition of IgE CSR by BCR
188 stimulation.

189
190 Two major outcomes of Syk-dependent BCR signaling are protein kinase C (PKC) activation and
191 Ca²⁺ flux. To examine the sufficiency of these pathways for IgE CSR inhibition we treated cells
192 with phorbol myristate acetate (PMA; a diacylglycerol analog that activates PKC) and/or
193 ionomycin (induces Ca²⁺ flux). PMA treatment led to a strong and dose-dependent reduction in
194 the representation of IgE cells, while, at all but the highest dose tested, IgG1 was either unaffected
195 or increased (Figure 4E). Meanwhile, the highest dose of ionomycin resulted in reductions in both
196 IgE and IgG1, with perhaps a somewhat stronger effect for IgE. The combined effect of PMA and
197 ionomycin together seemed mostly similar to the effect of stimulation with PMA alone. Overall,
198 these data suggest that PKC activation is sufficient to selectively inhibit IgE CSR, whereas Ca²⁺
199 signaling more broadly inhibits CSR to both IgE and IgG1.

200
201 **BCR stimulation acts synergistically with IL-21 or TGF β 1 to inhibit IgE CSR**
202 Having established that BCR signaling can substantially inhibit IgE CSR, we sought to determine
203 if its effects were synergistic with IL-21, which was previously identified as a critical negative
204 regulator of IgE *in vivo*.^{2,30} To this end, we activated B1-8i B cells *in vitro* with IL-4 and α CD40
205 and treated them with or without cognate antigen and IL-21 (or controls). The combination of
206 cognate antigen and IL-21 resulted in a greater reduction in IgE cells than either alone (Figure 5A,
207 left). Meanwhile, treatment with IL-21 alone or in combination with BCR ligands increased IgG1
208 cells as a fraction of class-switched cells (Figure 5A, right). These data reveal that BCR stimulation
209 and IL-21 can synergize to inhibit IgE, but not IgG1, CSR.

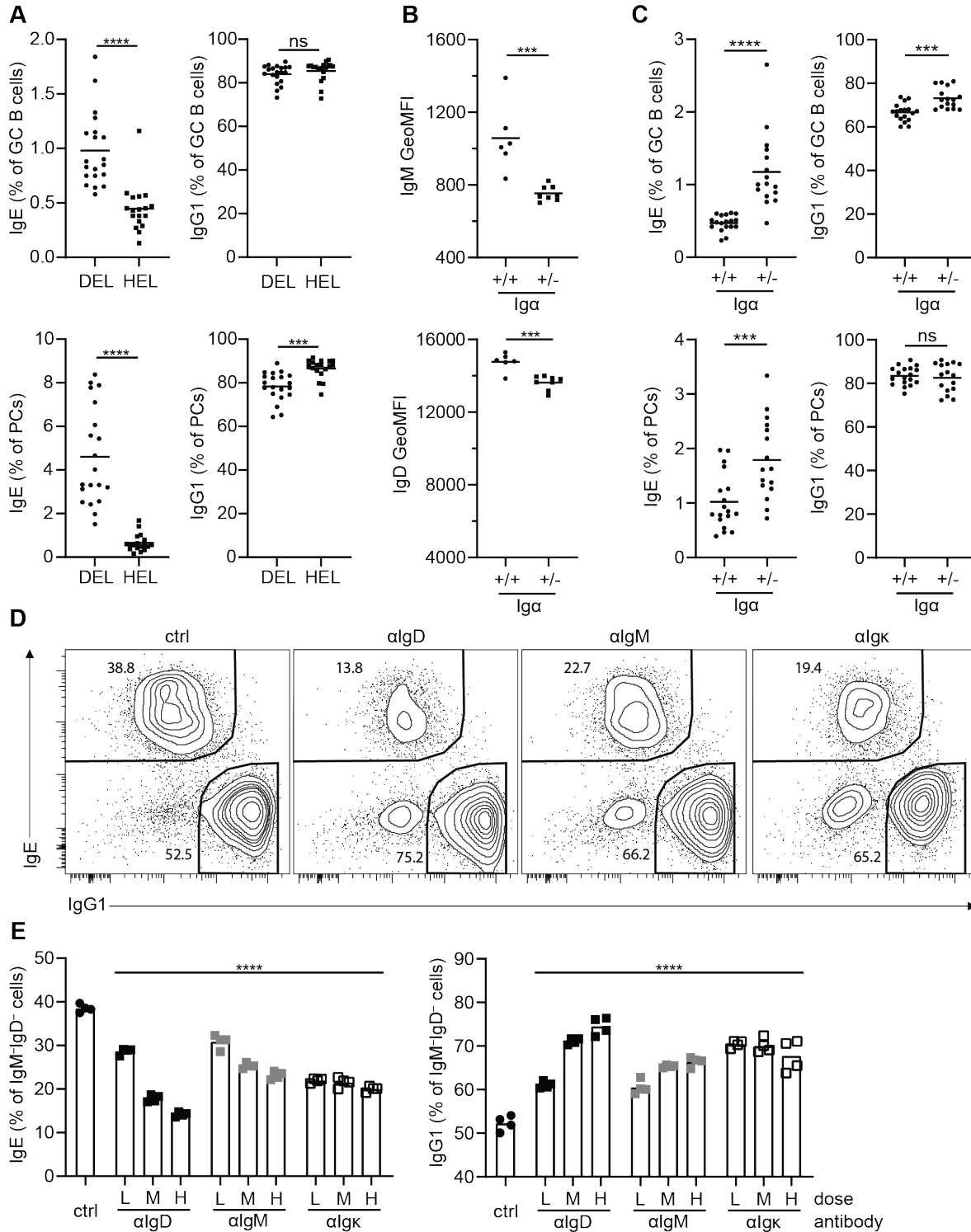
210
211 Having observed synergism between the inhibition of IgE CSR by BCR stimulation and IL-21, we
212 next sought to determine if TGF β 1 possessed similar synergistic capacity. Limited prior evidence
213 suggested that TGF β 1 could inhibit IgE CSR in mouse B cells.³¹ We observed that treatment with
214 TGF β 1 resulted in a dose-dependent reduction in the representation of IgE cells compared to a
215 slight increase in the representation of IgG1 cells (Figure S3A). However, as TGF β 1 is a
216 pleiotropic cytokine with effects on B cell survival and proliferation,³² it was unclear whether
217 TGF β 1 could directly inhibit IgE CSR. To resolve this question, as we previously reported for IL-
218 21² and for BCR ligation in Figure 3, we performed experiments with CTV. Culturing B cells with
219 TGF β 1 resulted in strongly reduced proliferation relative to control, evidenced by the substantially
220 larger fraction of cells that did not divide at all and the smaller fraction of cells that divided many
221 times (Figure S3B). Analyzing the rate of IgE and IgG1 switching at each cell division revealed
222 reductions for IgE, but not IgG1, in TGF β 1 treatment conditions, (Figure S3C). Finally, we
223 cultured B cells with α IgD or TGF β 1, alone or in combination, and observed that the combination
224 of both more strongly suppressed IgE than either alone (Figure 5B). These data are consistent with
225 a selective inhibition of IgE CSR by TGF β 1 that is synergistic with BCR stimulation.

226

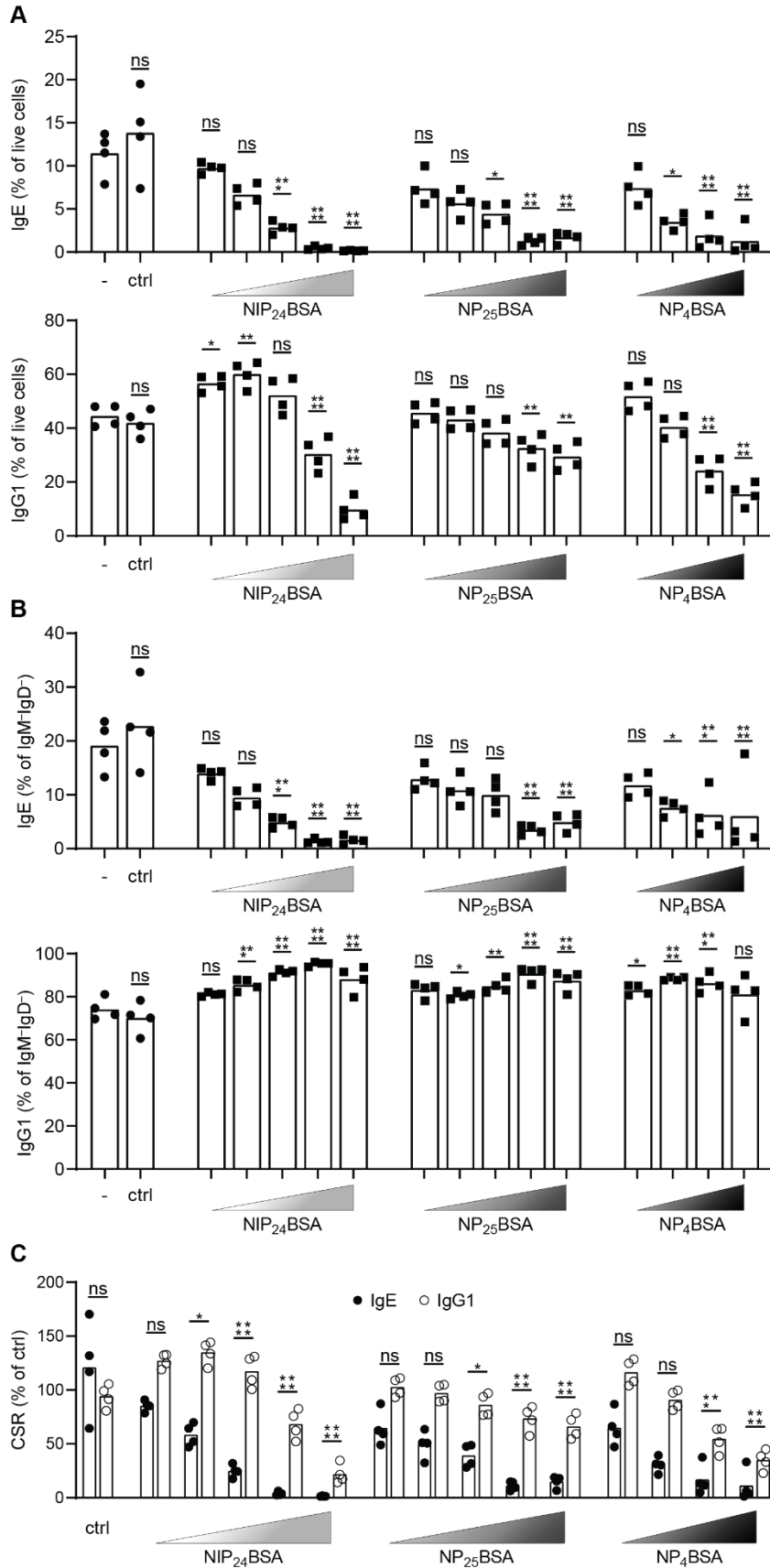
227 **BCR ligation inhibits IgE CSR in human cell culture**

228 Finally, we sought to translate our key findings to humans by investigating the inhibition of IgE
229 CSR by BCR stimulation of tonsillar B cells cultured in conditions that promote CSR to IgE, IgG1,
230 and IgG4. We observed that, similar to our results in mouse cell culture, α IgM treatment resulted
231 in an overall inhibition of CSR (Figure 6A). However, among class-switched cells, α IgM treatment
232 resulted in a dose-dependent reduction in the representation of IgE, but not IgG1 or IgG4, cells
233 (Figure 6B-C). These data are consistent with a selectively enhanced inhibition of IgE CSR relative
234 to IgG1 or IgG4. Next, we investigated the synergism between BCR stimulation and IL-21
235 treatment of human B cells and found that, as with mouse B cells, BCR ligation and IL-21 together
236 led to a greater reduction in IgE than either alone (Figure 6D). α IgM treatment and/or IL-21
237 treatment did not clearly affect IgG4, whereas the representation of IgG1 cells was enhanced by
238 IL-21 in a manner which was not affected by the presence/absence of α IgM. These findings support
239 the notion that BCR stimulation is a conserved, selective inhibitor of IgE CSR in mice and humans.

Figures

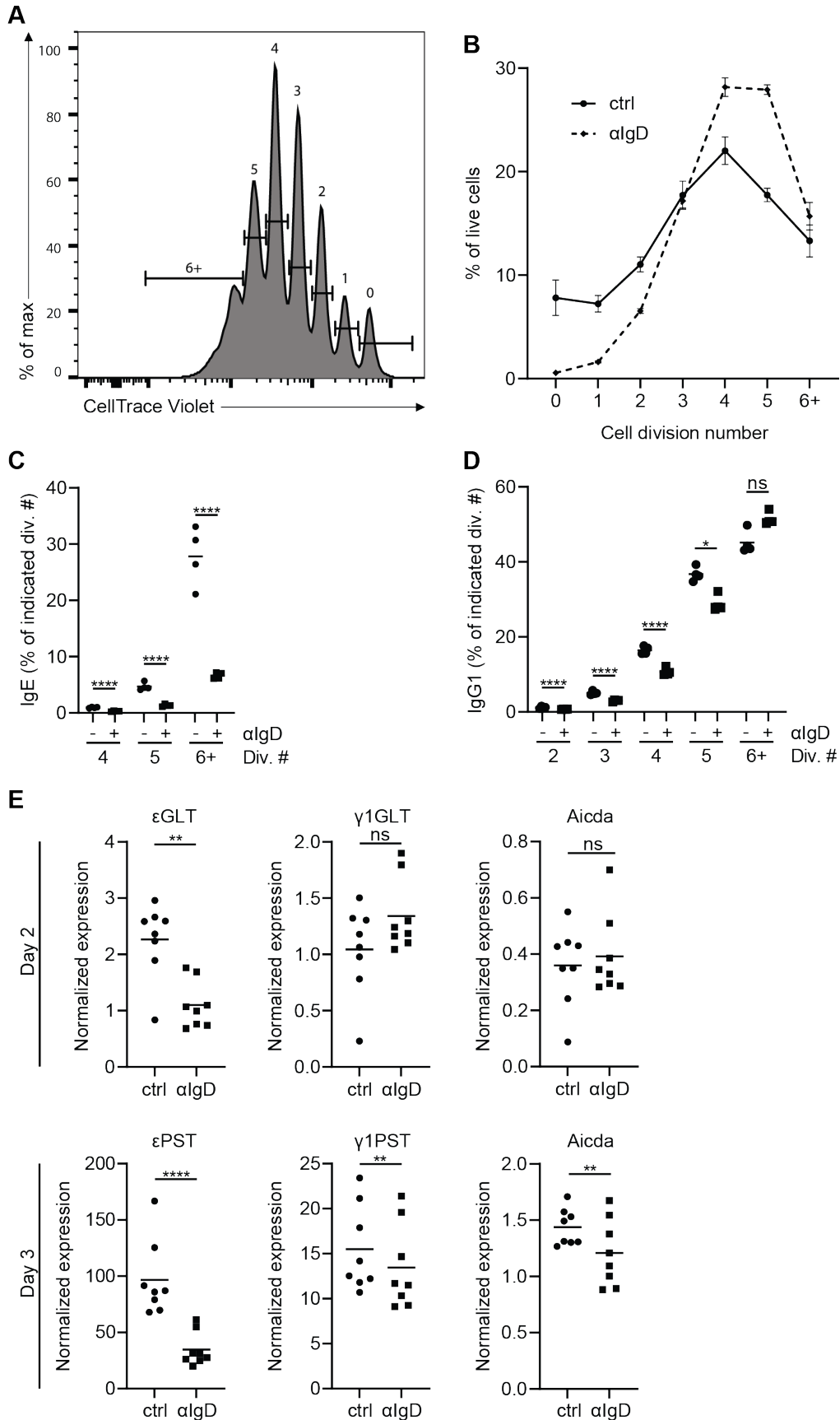


240 **Figure 1. BCR stimulation reduces the representation of IgE cells *in vivo* and *in vitro*.** (A)
241 Hy10 B cells were adoptively transferred into congenically-marked recipient mice that were then
242 immunized with ovalbumin-conjugated DEL or HEL in alum adjuvant. Shown are the proportions
243 of IgE cells (left column) and IgG1 cells (right column) within the GC (top row) and PC (bottom
244 row) compartments of transferred cells in the dLN at d7, quantified by flow cytometry. (B)
245 Quantification of surface IgM (top) and IgD (bottom) levels on follicular B cells from wildtype or
246 $Ig\alpha^{+/-}$ mice by flow cytometry. (C) Wildtype and $Ig\alpha^{+/-}$ mice were immunized subcutaneously with
247 NP-CGG in alum adjuvant and the resultant immune response in the dLN at d7 was analyzed by
248 flow cytometry. Plots are laid out as described for panel A. (D-E) Wildtype mouse B cells were
249 cultured with IL-4, α CD40, and the indicated treatments for 4 days prior to analysis by flow
250 cytometry. (D) Representative flow cytometry plots of IgE and IgG1 staining among class-
251 switched (IgM^-IgD^-) cells according to treatment condition (from left to right; ctrl [GGG], α IgD,
252 α IgM, α Ig κ ; all at 1 μ g/mL). (E) Quantification of the effects of treatment with low (L; 100 ng/mL),
253 medium (M; 300 ng/mL), or high (H; 1 μ g/mL) doses of α IgD (black squares), α IgM (grey
254 squares), α Ig κ (white squares), or ctrl (GGG; 1 μ g/mL; black circles) antibodies on the proportions
255 of IgE (left) and IgG1 (right) cells among class-switched (IgM^-IgD^-) cells. (A-C, E) Dots represent
256 samples from individual mice and bars represent the mean values. ns, not significant; *, $P < 0.05$;
257 **, $P < 0.01$; ***, $P < 0.001$; ****, $P < 0.0001$ (unpaired t test [A-C], one-way repeated measures
258 ANOVA [E] with Dunnett's post-test comparing each condition to the control with the Holm-
259 Sidak correction for multiple comparisons). Results are pooled from three (A) or two (B, C, E)
260 independent experiments or are representative of two independent experiments (D).



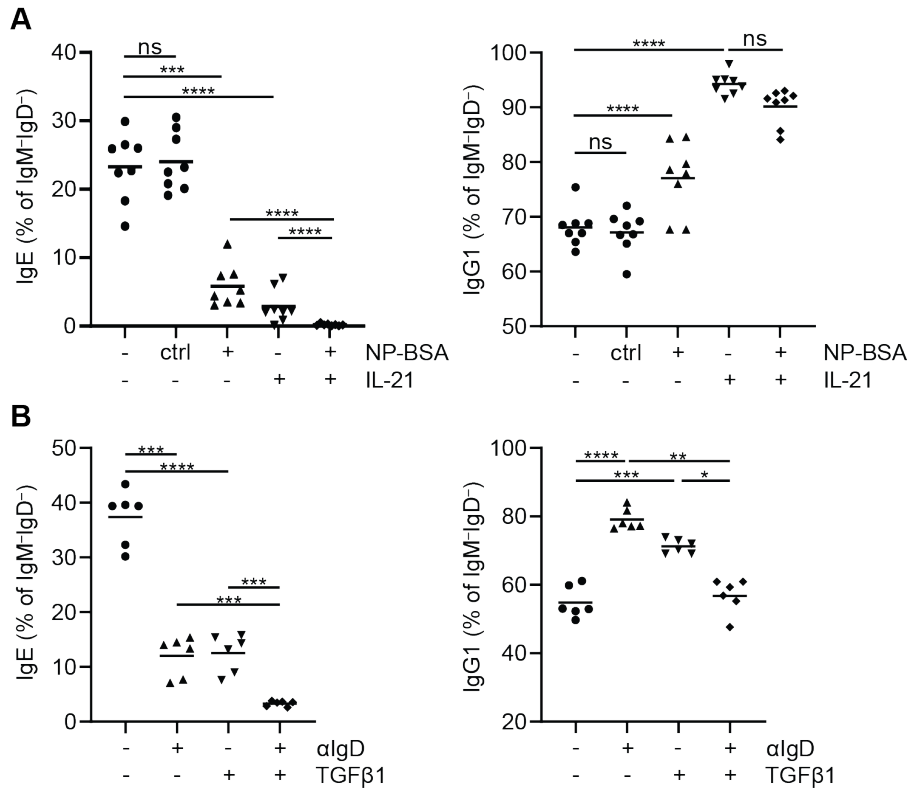
261
262
263
264
265
266
267
268
269
270
271
272
273
274
275
276

Figure 2. B cell culture with cognate antigen reduces yields of IgE cells. (A-C) Purified B1-8i B cells were cultured with IL-4 and α CD40 for 4 days with control ('-' is no treatment, 'ctrl' is BSA at 50 ng/mL; black circles) or cognate antigen (NIP₂₄BSA, NP₂₅BSA, or NP₄BSA; black squares) prior to analysis by flow cytometry. Doses of cognate antigen ascend from left to right as represented by the gradient triangles, exact doses are as follows (ng/mL): NIP₂₄BSA; 0.002, 0.005, 0.015, 0.05, 0.25 | NP₂₅BSA; 0.016, 0.08, 0.4, 2, 10 | NP₄BSA; 20, 200, 1.25×10^3 , 1×10^4 . (A-B) Quantification of the proportion of IgE (top) or IgG1 (bottom) cells among all live cells (A) or within the class-switched (IgM⁻IgD⁻) compartment (B) as assessed by flow cytometry. (C) Quantification of the frequency of IgE cells (black circles) and IgG1 cells (white circles) among live cells in the antigen-treated condition as a fraction of their frequency among live cells in the control condition. (A-C) Dots represent samples from individual mice and bars represent the mean values. ns, not significant; *, P < 0.05; **, P < 0.01; ***, P < 0.001; ****, P < 0.0001 (one-way repeated measures ANOVA with Dunnett's post-test comparing each condition to the untreated control with the Holm-Sidak correction for multiple comparisons). Results are representative of two independent experiments.



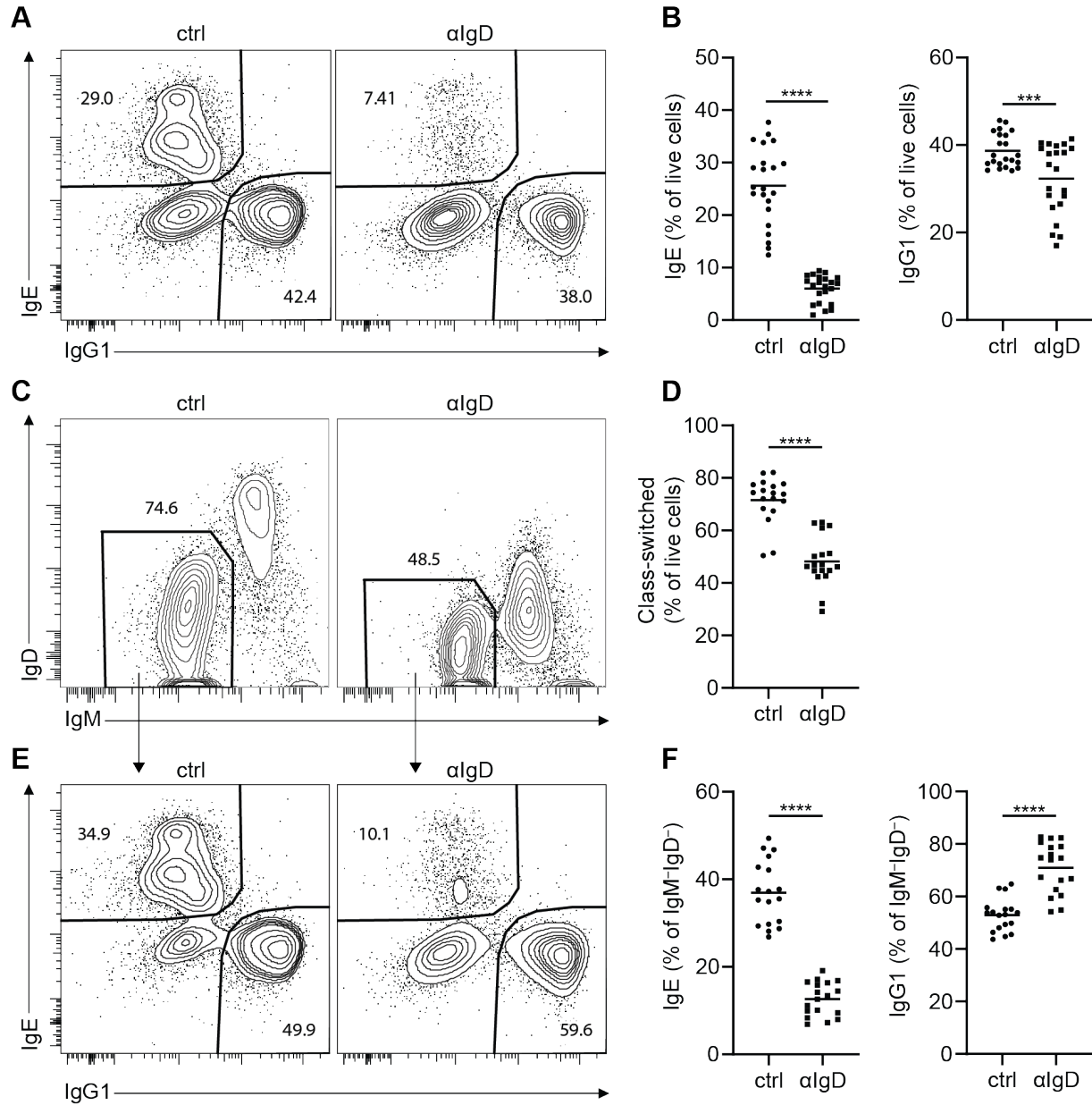
277 **Figure 3. BCR stimulation inhibits IgE CSR.** (A-D) Purified naïve mouse B cells were loaded
278 with CTV (see Methods) and then cultured for 4 days with IL-4, α CD40, and control (GGG) or
279 α IgD antibodies (3 μ g/mL) prior to analysis by flow cytometry. (A) Representative histogram from
280 the control-treated condition showing CTV staining and cell division number gating. (B)
281 Quantification of the frequency (%) of live cells at each cell division for control- and α IgD-treated
282 conditions, n=4. (C-D) Quantification of the proportion of IgE (C) and IgG1 (D) cells among live
283 cells within each cell division (gated as shown in panel A) for control (black circles) and α IgD
284 (black squares) treatments. (E) Purified naïve mouse B cells were cultured with IL-4, α CD40, and
285 the indicated treatments for two (top row) or three (bottom row) days prior to quantification of the
286 indicated transcripts by RT-qPCR; numbers on the y axis are relative arbitrary units normalized to
287 HPRT. Dots represent average values (B), or samples from individual mice (C-E). Error bars show
288 the SEM (B). Bars represent the mean values (C-E). ns, not significant; *, P < 0.05; **, P < 0.01;
289 ****, P < 0.0001 (one-way repeated measures ANOVA with Dunnett's post-test comparing the
290 indicated pairs of conditions with the Holm-Sidak correction for multiple comparisons [C-D],
291 paired t test [E]). Results are representative of five similar experiments (A-D) or are pooled from
292 three independent experiments (E).

293 **Figure 4. BCR stimulation represses IgE CSR via Syk-dependent rather than p110δ-**
294 **dependent signaling.** (A-E) Purified B cells were cultured with IL-4 and α CD40 for 4 days under
295 various conditions of stimulation and/or inhibitor treatment (as indicated on the x axes) prior to
296 analysis by flow cytometry. (A) Quantification of the proportion of IgE cells among class-switched
297 (IgM⁻IgD⁻) cells according to treatment with α IgD or ctrl (GGG) at 1 μ g/mL, as well as different
298 doses of nemiralisib (L – 25nM, M – 100nM, H – 250nM) or vehicle control (DMSO). (B)
299 Normalization was performed by dividing the frequency of IgE cells among class-switched (IgM⁻
300 IgD⁻) cells in the α IgD-treated (3 μ g/mL) condition by their frequency in the control-treated
301 condition (GGG; 1 μ g/mL), for each dose of nemiralisib. (C) Quantification of the proportion of
302 IgE cells among class-switched cells treated with α IgD (1 μ g/mL; +) or control (no treatment; –),
303 in the presence of vehicle (veh; DMSO) or different doses of inhibitors of Syk (PRT062607, L –
304 0.4 μ M, M - 1 μ M, H – 2.5 μ M), Btk (ibrutinib; L – 1nM, M – 10nM, H – 50nM), all p110 isoforms
305 and mTOR (omipalisib; L – 1nM, M – 5nM, H – 10nM), p110 δ (idelalisib; L – 10nM, M – 50nM,
306 H – 250nM), or all PI3K isoforms (wortmannin; L – 40nM, H – 200nM). See Supplementary Table
307 1 for statistical comparisons. (D) Quantification, for each dose of inhibitor or vehicle control
308 described for panel D, of the frequency of IgE cells among class-switched (IgM⁻IgD⁻) cells in the
309 α IgD-treated condition as a percentage of their frequency in the untreated control condition. (E)
310 Quantification of the frequency of IgE (left) or IgG1 (right) cells among live cells following
311 treatment with the indicated doses (in ng/mL) of PMA and/or ionomycin. Dots represent samples
312 from individual mice and bars represent the mean values. ns, not significant; *, P < 0.05; **, P <
313 0.01; ***, P < 0.001; ****, P < 0.0001 (one-way repeated measures ANOVA [A-E] with Dunnett's
314 post-test comparing the indicated pairs of conditions [A-B], the α IgD-treated condition [D], or the
315 vehicle control [E] using the Holm-Sidak correction for multiple comparisons). See
316 Supplementary Table 1 for statistics for panel C. Results are representative (A, C-E) or pooled
317 from (B) two independent experiments.

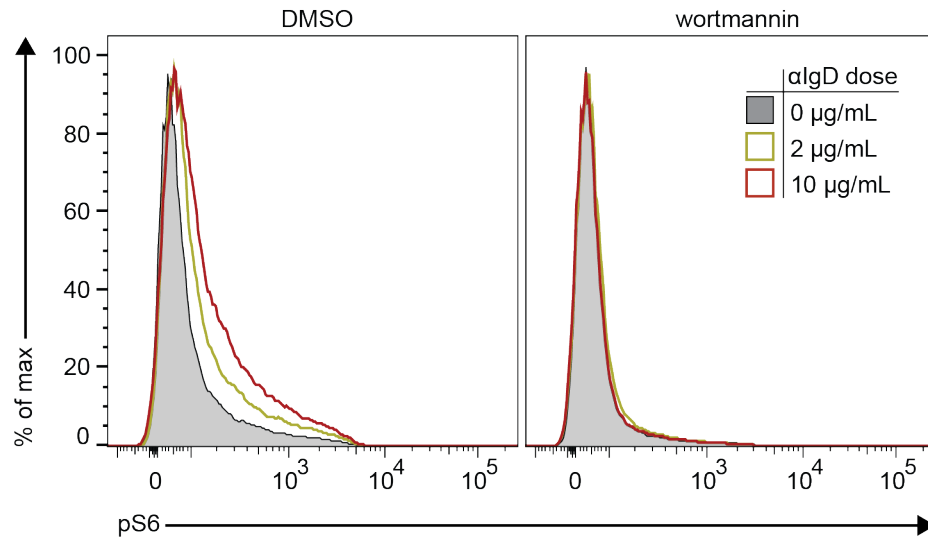


318 **Figure 5. B cell receptor stimulation acts synergistically with IL-21 or TGFβ1 to inhibit IgE**
 319 **CSR.** (A) Purified B1-8i B cells were cultured for four days with IL-4, αCD40, and cognate
 320 antigen (NP-BSA – 10 ng/mL) or control antigen (ctrl, BSA – 10 ng/mL) in the presence or
 321 absence of IL-21 (25 ng/mL). The frequencies of IgE and IgG1 cells among class-switched
 322 (IgM⁺IgD⁻) cells were quantified by flow cytometry. (B) Purified B cells were cultured for four
 323 days with or without αIgD (3 μg/mL) and in the presence or absence of TGFβ1 (2 ng/mL). The
 324 frequencies of IgE and IgG1 cells among class-switched cells were quantified by flow cytometry.
 325 (A-B) Dots represent samples from individual mice and bars represent the mean. ns, not
 326 significant; *, p < 0.05; **, p < 0.01; ***, p < 0.001; ****, P < 0.0001 (one-way repeated
 327 measures ANOVA with Dunnett's post-test comparing the indicated pairs of conditions with the
 328 Holm-Sidak correction for multiple comparisons). Results are pooled from two independent
 329 experiments.

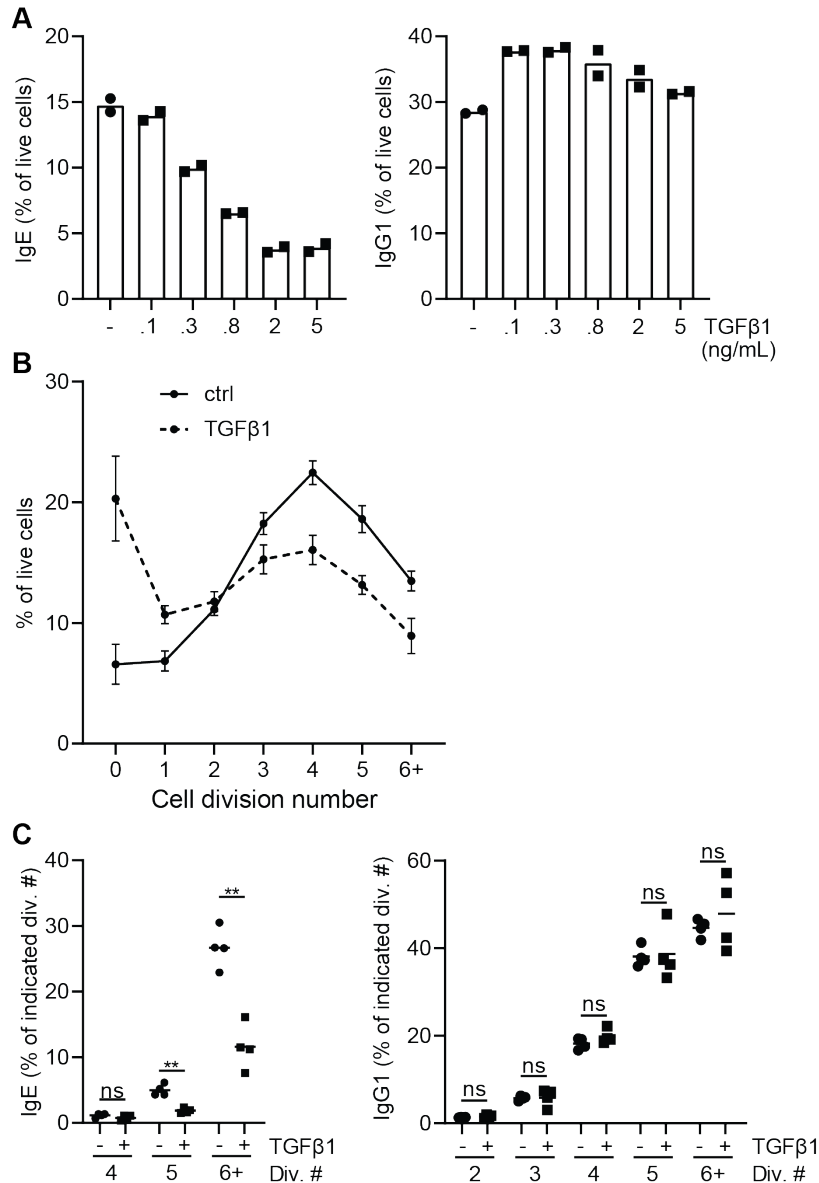
330 **Figure 6. BCR stimulation inhibits IgE CSR in human B cells.** (A-D) Purified human tonsillar
331 naïve B cells were cultured in IL-4, IL-10, α CD40, and the indicated treatment conditions for 8
332 days prior to analysis by flow cytometry. (A-B) Representative flow cytometry plots and gating
333 strategies for class-switched (IgM⁻IgD⁻) cells (A), IgE cells (B; top row), or IgG1 and IgG4 cells
334 (B; bottom row) for cells treated with low, medium, or high (0.1, 0.3, or 3 μ g/mL, respectively)
335 doses of α IgM or control (GGG; 3 μ g/mL). Cells in (B) were pre-gated as IgM⁻IgD⁻, as shown in
336 (A). Note that the IgG1 antibody cross-reacts with IgG4 and therefore IgG4-expressing cells
337 appear as IgG4⁺ IgG1⁺, whereas IgG1-expressing cells appear as IgG4⁻ IgG1⁺. (C-D) The
338 proportions of IgE (left), IgG1 (center), and IgG4 (right) cells within the class-switched (IgM⁻IgD⁻
339) compartment were quantified by flow cytometry according to the indicated treatment conditions.
340 (C) Quantification of the impact of α IgM titration on CSR. Treatment doses were as described for
341 panels A-B. (D) Quantification of the synergistic impacts of IL-21 and BCR ligation on CSR.
342 Treatment doses were: ‘-’ – untreated; ctrl – GGG at 300 ng/mL (grey) or 2 μ g/mL (black), α IgM
343 – 300 ng/mL (grey) or 2 μ g/mL (black); IL-21 – 5 (grey) or 10 (black) ng/mL. (C-D) Dots represent
344 samples from individual human tonsil donors and bars represent the mean. ns, not significant; *, P
345 < 0.05; **, P < 0.01; ***, P < 0.001; ****, P < 0.0001 (one-way repeated measures ANOVA with
346 Dunnett’s post-test comparing the indicated pairs of conditions and the Holm-Sidak correction for
347 multiple comparisons). Results are representative of (A-B) or pooled from (C-D) two experiments.



348 **Figure S1. Supporting data for Figure 1.** (A-F) B cells were cultured with IL-4 and α CD40 for
349 4 days prior to analysis by flow cytometry with control (GGG, 3 μ g/mL) or α IgD (3 μ g/mL)
350 antibodies. (A-B) Representative flow cytometry plots (A) and quantification (B) of the impact of
351 BCR ligation on the frequency of IgE and IgG1 cells among live cells. (C-D) Representative flow
352 cytometry plots (C) and quantification (D) of the impact of BCR ligation on the frequency of class-
353 switched (IgM⁻IgD⁻) cells among live cells. (E-F) Representative flow cytometry plots (E) and
354 quantification (F) of the impact of BCR ligation on the frequency of IgE and IgG1 cells among
355 class-switched (IgM⁻IgD⁻) cells. (B, D, F) Dots represent samples from individual mice and bars
356 represent the mean values. ***, P < 0.001; ****, P < 0.0001 (paired t test). Results are
357 representative of six (A) or five (C, E), or are pooled from six (B) or five (D, F), independent
358 experiments.



359 **Figure S2. Supporting data for Figure 4.** Cultured B cells were treated with the indicated dose
360 of α IgD and with either 200nM wortmannin or DMSO vehicle control prior to analysis of
361 phosphorylated S6 (pS6) by phosflow (see Methods). Data are representative of two independent
362 experiments.



363 **Figure S3. TGFβ1 inhibits IgE class switching.** (A-C) Purified naïve B cells were loaded with
 364 CTV (see Methods) and then cultured for 4 days with IL-4, αCD40, and vehicle control (DMSO)
 365 or TGFβ1 prior to analysis by flow cytometry. (A) The rate of switching to IgE (left) or IgG1
 366 (right) in B cell culture according to TGFβ1 dose. (B) Quantification of the percentage of live cells
 367 at each cell division for control- and TGFβ1-treated conditions, n=4. (C) Quantification, for each
 368 of the indicated cell divisions, of the frequency of IgE (left) and IgG1 (right) cells among live cells,
 369 according to treatment group (control, black circles; αIgD, black squares). TGFβ1 doses were 0 or
 370 2 ng/mL (– or +, respectively). (A,C) Dots represent samples from individual mice and bars
 371 represent the mean. (B) Dots represent the mean, errors bars show the SEM. ns, not significant;
 372 **, p<0.01 (one-way repeated measures ANOVA with Dunnett’s post-test comparing the indicated
 373 pairs of conditions with the Holm-Sidak correction for multiple comparisons). Except for panel A,
 374 results are representative of two independent experiments.

375 Discussion

376 Here, we report that BCR stimulation selectively inhibits CSR to IgE in mouse and human B cells.
377 In mice, the representation of IgE cells in PC and GC compartments was inversely regulated by
378 BCR affinity and surface expression. We relate these findings to the inhibition of IgE CSR by
379 finding reduced ϵ GLT and fewer IgE-switched cells across cell divisions in cells stimulated
380 through their BCRs versus those left untreated. A major finding is that the selective inhibition of
381 IgE CSR by BCR signaling required Syk, rather than PI3K as had been proposed, and could be
382 mimicked by the activation of PKC. BCR stimulation synergized with IL-21 or TGF β 1 to inhibit
383 IgE CSR more greatly than with any one stimulus alone. Finally, we replicated our findings from
384 murine studies of selective inhibition of IgE CSR by BCR stimulation as well as synergy for IgE
385 CSR inhibition by IL-21 and BCR stimulation in cultures of human tonsillar B cells. These
386 observations establish that IgE CSR is uniquely susceptible to inhibition by BCR signaling.

387
388 The present work extends our understanding of the inhibition of IgE CSR by BCR stimulation.
389 Prior work left unclear whether BCR stimulation had a broad effect on CSR^{6,7} or a selective effect
390 on IgE¹¹. Furthermore, while prior studies exclusively used antibodies to stimulate the BCR,^{5-7,33}
391 we additionally included data with cognate antigen *in vitro* and *in vivo*. These experiments allowed
392 us to examine if different cognate antigens exhibited different selectivity for IgE versus IgG1 CSR
393 inhibition. While all variants we tested resulted in greater inhibition of IgE than IgG1 CSR, some
394 intermediate doses exhibited exquisite specificity for IgE whereas high doses could strongly
395 reduce both IgE and IgG1. Interestingly, low doses of high-affinity high-valency antigen actually
396 resulted in increased IgG1 CSR relative to control, which may relate to a prior report that identified
397 increased IgG1 switching in LPS culture with high-affinity antigen.³⁴ A similar finding was also
398 reported for IgA.³⁵ Meanwhile, we identified no conditions under which BCR ligation resulted in
399 increased IgE, reinforcing our observations of selective IgE CSR inhibition by BCR stimulation.

400
401 Our qPCR results indicate that a likely mechanism for the selective inhibition of IgE CSR by BCR
402 stimulation is a reduction in ϵ GLT. This finding contrasts with earlier work exploring the
403 mechanism by which BCR stimulation inhibited CSR, which did not observe effects on ϵ GLT.⁶
404 One key difference in our studies was in the timepoint analyzed: we measured ϵ GLT at day 2,
405 which we have found is a key timepoint prior to CSR,² whereas Jabara *et al.*⁶ analyzed ϵ GLT at
406 day 4, a timepoint at which we have found CSR has already occurred. Our quantitative analysis
407 may also have been more sensitive in detecting the reduction in ϵ GLT. Rather than ϵ GLT, prior
408 work focused on a temporary, BCR stimulation-induced reduction in *Aicda* expression as a
409 potential mechanism for CSR inhibition.^{6,7} However, a series of studies from a different group^{5,33}
410 found that, while BCR stimulation reduced AID, AID overexpression actually reduced IgE CSR.
411 Overall, there is no consistent link between changes in AID protein or gene expression and IgE
412 CSR following BCR ligation. Here, we found that *Aicda* transcripts were unchanged relative to
413 control at day 2 after BCR stimulation and were slightly reduced at day 3. For IgE, the more
414 substantial and earlier BCR ligation-induced reduction in ϵ GLT relative to *Aicda*, in addition to
415 aforementioned evidence^{5,33}, indicates that differences in ϵ GLT levels represent a more plausible
416 explanation for strongly reduced CSR. Relating to the broad effects of BCR signaling on CSR
417 under some conditions, our findings do not exclude a role for alterations in AID gene or protein
418 expression.

419

420 Using various inhibitors, we establish a Syk-dependent rather than p110 δ -dependent signaling
421 mechanism for the inhibition of IgE CSR by BCR stimulation. Our observations of the lack of a
422 strong rescue of IgE CSR with the pan-p110/mTOR inhibitor omipalisib, or the lack of any rescue
423 with the pan-p110 inhibitor wortmannin, in the face of BCR stimulation were unexpected given a
424 prior report that a PI3K $\alpha/\delta/\beta$ inhibitor completely rescued IgG1 CSR from inhibition by BCR
425 stimulation.⁷ This difference in the extent of CSR rescue for IgE and IgG1 might indicate that
426 BCR-dependent effects on IgG1 CSR are moreso driven by PI3K signaling, whereas we have
427 shown that BCR-dependent effects on IgE CSR require Syk-dependent signaling pathways. This
428 model might also help to explain the selectively enhanced impact of BCR stimulation on IgE
429 switching relative to IgG1. Alternatively, it could be that a maximal blockade of PI3K is required
430 to observe an effect on BCR ligation-induced IgE CSR inhibition, and that this maximal blockade
431 cannot be achieved with chemical inhibitors due to the necessity of PI3K signaling for B cell
432 survival.³⁶ However, at least for wortmannin, this possibility seems less likely as we found that
433 200nM (a dose comparable to that previously observed to effectively inhibit primary mouse B cell
434 chemotaxis)³⁷ was sufficient to completely block detectable BCR ligation-induced S6
435 phosphorylation, consistent with a complete blockade of PI3K activity (Figure S2). In addition to
436 our studies with inhibitors, we used PMA and ionomycin to bypass the BCR and demonstrate that
437 PKC activation, and, to a lesser extent, Ca²⁺ signaling, were sufficient to inhibit IgE CSR, with
438 PKC activation having a more selective effect on IgE. Overall, we find greater evidence that the
439 inhibition of IgE CSR depends on a Syk-Btk signaling axis than PI3K.

440
441 While we did not find a role for PI3K signaling in the inhibition of IgE CSR by antigen-induced
442 BCR signaling, several PI3K inhibitors had clear impacts on baseline IgE switching, consistent
443 with prior reports.^{16,20} The mechanism underlying the impact of these inhibitors on IgE CSR
444 remains unclear, including whether the inhibitors are modifying PI3K activity related to antigen-
445 independent (tonic) BCR signaling, such as that which is required for B cell survival, or PI3K
446 signaling downstream of other pathways entirely. Interestingly, observations of p110 inhibitors
447 increasing baseline switching to IgE in murine cell culture may not translate to humans, as
448 inhibition of p110 δ was reported to reduce, rather than increase, IgE in cultured human B cells.³⁸
449 If confirmed, this would suggest that PI3K activity might differently regulate IgE CSR in non-
450 BCR stimulated human versus mouse B cells.

451
452 Our finding of synergy between BCR signaling and IL-21 for the inhibition of IgE CSR may be
453 particularly important *in vivo*. In a physiologic response, B cells possess a variety of starting
454 affinities for cognate antigen, and multiple antigens may be present in varying amounts. Our data
455 suggests that lower-affinity B cells, or B cells responding to a scarcer antigen, may be relatively
456 advantaged for IgE CSR, as they would experience weaker or fewer BCR signaling events relative
457 to high-affinity cells responding to abundant antigen. Varying antigen encounters would also have
458 ramifications for subsequent T:B interactions, as B cells that bind greater amounts of antigen
459 would not only have greater BCR signaling but also greater antigen capture. Greater antigen
460 capture, leading to more antigen presentation, could potentially influencing the nature of help
461 received from T follicular helper cells (T_{FH}), which are notably important sources of IL-21 and IL-
462 4.^{1,39} Therefore, our findings imply that IgE CSR may be more likely to occur in lower-affinity B
463 cells engaged with T_{FH} producing less IL-21 but ample IL-4.^{1,40} We also found that TGF β 1
464 treatment inhibited IgE CSR and could synergize with BCR ligation. Importantly, we found that,
465 although TGF β 1 globally limited B cell proliferation, it also resulted in a selective reduction in

466 IgE at each cell division, consistent with IgE CSR inhibition. The timing of TGF β 1 signaling
467 related to B cell activation *in vivo* is perhaps less clear than for IL-21 or BCR ligation, but activated
468 B cells have been described to undergo autocrine TGF β 1 signaling critical for maintaining immune
469 tolerance,⁴¹ indicating that B cell activation is associated with TGF β 1 signaling that could restrict
470 IgE CSR.

471
472 Our finding that BCR stimulation also impaired human IgE CSR provides an important piece of
473 translational evidence for this topic, which until now was restricted to mouse studies. We found
474 that α IgM resulted in similar inhibition of IgE CSR in human cells to that which we observed in
475 mouse cells. It will be interesting to determine in the future if the inhibition of IgE CSR by BCR
476 stimulation in human cells is Syk-dependent, as we observed in mouse B cells. Notably, there are
477 clear links between human mutations that impair antigen-receptor signaling and elevated IgE or
478 atopy.⁴² However, in addition to potential impacts on B cell CSR, alterations in antigen receptor
479 signal transduction could affect T cells, IgE B cells,^{8,10} and/or IgE PCs;³ therefore, it will be
480 important to disentangle the contributions made by each cell type to allergic disease pathogenesis.

481
482 This study defines ligand-induced BCR signaling as a selective, negative regulator of IgE CSR in
483 mouse and human B cells. Our finding that BCR signaling and specific cytokines (IL-21 or
484 TGF β 1) synergized to inhibit IgE CSR reveals how multiple layers of regulation can cooperate to
485 suppress the development of allergic immunity. This raises the question of whether the
486 development of allergy is associated with signaling impairments downstream of the BCR and/or
487 cytokine receptors that normally inhibit IgE CSR. Overall, we believe that our findings are of
488 significance for understanding the homeostatic regulation of allergic immunity, with implications
489 for allergic disease pathogenesis.

490 **Methods**

491 *Mice and immunizations*

492 All mice used for experiments in this study were on a C57BL/6 (B6) background (backcrossed
493 ≥ 10 generations). Mice for experiments were sex and age-matched between groups as much as
494 possible and both male and female mice were used. For *in vivo* experimentation, mice were at least
495 6 weeks of age and for *in vitro* experimentation donor animals were at least 5 weeks of age. Mice
496 were housed in specific-pathogen-free facilities. Mouse work was approved by the Institutional
497 Animal Care and Use Committee (IACUC) of the University of California, San Francisco (UCSF).

498
499 B1-8i (012642; B6.129P2(C)-*Igh*^{tm2Cgn}/J), Boy/J (002014; B6.SJL-*Ptprc*^a*Pepc*^b/BoyJ), B6/J
500 (000664; C57BL/6J), and B6 Thy1.1 (000406; B6.PL-*Thy1*^a/CyJ) mice were originally from The
501 Jackson Laboratory and were maintained in our colony. B6/J, Boy/J, and B6 Thy1.1 mice were
502 used as “WT” throughout. Immunizations consisted of antigen dissolved in D-PBS and mixed
503 50:50 volumetrically with alum (Alhydrogel; Accurate Chemical and Scientific) injected in a
504 volume of 20 μ L subcutaneously into the ear pinnae. For immunization of Hy10 recipients in Figure
505 1A, 6.25 μ g DEL-OVA or HEL-OVA was used (see *HEL-OVA/DEL-OVA preparation* below). For
506 immunization of wildtype and *Ig* α ^{+/-} mice in Figure 1B-C, 10 μ g NP conjugated to chicken gamma
507 globulin (NP-CGG; Biosearch Technologies) was used. The left and right facial LNs were pooled
508 for analysis at endpoint (d7) by flow cytometry.

509

510 *HEL-OVA/DEL-OVA preparation*

511 HEL/DEL-OVA conjugations were carried out as using maleimide thiol chemistry as described
512 previously.¹⁰ Correct product formation was verified with SDS-PAGE. Finally, products were
513 separated from reactants by FPLC, enrichment was assessed using SDS-PAGE, and concentration
514 was determined by A₂₈₀.

515

516 *Mouse cell culture, in vitro BCR stimulation, and inhibitor treatments*

517 All *in vitro* mouse cell culture experiments (except phosflow experiments, see below) were
518 performed with either total (Figures 1, 3, 4, and 5B), or *Ig* κ -negative (Figures 2 and 5A) B cells,
519 purified by negative selection as described previously.³ After purification, cells were resuspended
520 in complete RPMI (cRPMI), composed of RPMI 1640 without L-glutamine (Thermo Fisher
521 Scientific), 10% FBS, 10 mM Hepes, 1X penicillin streptomycin L-glutamine (Thermo Fisher
522 Scientific), and 50 μ M β -mercaptoethanol (Thermo Fisher Scientific). Purified B cells were seeded
523 at a density of 2-10 * 10³ cells per well in 96-well Microtest U-bottom plates (BD Falcon) and
524 were cultured with α CD40 (150 ng/mL; clone FGK-45; Miltenyi Biotec) and IL-4 (25 ng/mL;
525 Peprotech) for prior to analysis by flow cytometry (d4) or RT-qPCR (d2-3). Cells were plated in
526 triplicate for each condition, except for some CTV experiments where sextuplicates were used. In
527 some cases, CD45-congenic B cells were co-plated to allow the combined assessment of cells from
528 two different mice.

529

530 BCR stimulation with antibodies was performed using goat anti-mouse IgD (Nordic MUBio), goat
531 polyclonal F(ab')₂ anti-mouse *Ig* κ (LifeSpan Biosciences), goat polyclonal F(ab')₂ anti-mouse
532 *Ig*M (α *Ig*M; Jackson ImmunoResearch), or Chrompure Goat *Ig*G (Jackson ImmunoResearch) as a
533 control. BCR stimulation with cognate antigen was performed using NP(4)BSA (Biosearch
534 Technologies), NP(25)BSA (Biosearch Technologies), NIP₂₄BSA (Biosearch Technologies), or
535 BSA (Sigma-Aldrich) as a control. Recombinant human TGF β 1 (Peprotech) was used for

536 experiments in Figure 5. Stimulations were prepared in the culture medium at the doses indicated
537 in figure legends. All inhibitors were diluted in DMSO. The concentration of DMSO in culture
538 never exceeded 0.1% and was typically lower. The specific DMSO vehicle control concentration
539 in each experiment was made to be equivalent to the highest concentration of DMSO in any
540 inhibitor-treated well. See figure captions for specific inhibitors and concentrations used.

541

542 *CellTrace Violet labeling*

543 Labeling with CellTrace Violet (CTV; Life Technologies Corporation) was performed as
544 described previously.² Briefly, cells were incubated with CTV at 1 μ M for 20 minutes in a 37°C
545 water bath and then washed twice with FBS (Life Technologies Corporation) underlaid in each
546 wash step. Pilot experiments revealed that CTV labeling and associated centrifugation steps
547 resulted in a ~75% reduction in cell number, which was taken into account when plating cells after
548 labeling.

549

550 *RNA extraction, cDNA conversion, and RT-qPCR amplification*

551 Harvesting of nucleic acids, the preparation of cDNA, and RT-qPCR amplification, standard curve
552 preparation, and analysis were performed as described previously.² The following specific primers
553 were used for the qPCR assays:

554 ϵ GLT forward: 5'-TCGAATAAGAACAGTCTGGCC-3'

555 ϵ GLT reverse: 5'-TCACAGGACCAGGGAAGTAG-3'

556 γ 1 GLT forward: 5'-CAGGTTGAGAGAACCAAGGAAG-3'

557 γ 1 GLT reverse: 5'-AGGGTCACCATGGAGTTAGT-3'

558 *Aicda* forward: 5' CCTAAGACTTTGAGGGAGTCAA-3'

559 *Aicda* reverse: 5'-CACGTAGCAGAGGTAGGTCTC-3'

560 *Hprt* (internal control) forward: 5'-TGACACTGGCAAACAATGCA-3'

561 *Hprt* (internal control) reverse: 5'GGTCCTTTTCACCAGCAAGCT-3'

562

563 *Human samples, B cell purification, and cell culture*

564 Human B cells were purified from tonsils fractions obtained from UCSF pathology. Excess tissue
565 collected following routine tonsillectomies was completely de-identified, allowing samples to not
566 be classified as human subjects research according to the guidelines from the UCSF Institutional
567 Review Board. Tonsillar tissue was dissociated, a single cell suspension was prepared and then
568 cells were cryopreserved as described previously.⁴³ Naive B cells were purified by magnetic bead
569 depletion using the MojoSort Human Naive B Cell Isolation kit (BioLegend) according to
570 manufacturer's instructions but with some additional modifications as previously described.²
571 Following purifications, naïve human B cells were resuspended in complete Iscove's modified
572 Dulbecco's medium (cIMDM), consisting of: IMDM supplemented with GlutaMAXTM (Gibco),
573 10 % FBS, 1X penicillin-streptomycin (UCSF Cell Culture Facility), 1X insulin-transferrin-
574 selenium (ITS-G, Fiser Scientific), 0.25 μ g/mL Amphotericin B (Neta Scientific), and 100 IU/mL
575 Nystatin (Neta Scientific).

576

577 A fraction of purified cells was analyzed by flow cytometry to verify purity. Cells were then
578 cultured at a density of 5-20k live B cells/well in 96-well Microtest U-bottom plates (BD
579 Falcon) for 8 days with 100 ng/mL anti-human CD40 antibody (clone G28.5; Bio-X-Cell), 25
580 ng/mL recombinant human IL-4 (Peprotech), and 50 ng/mL human IL-10 (Peprotech). Where

581 indicated in the figure caption, 50 ng/mL human IL-21 (Peprotech), goat anti-human IgM F(ab')₂
582 fragments, or GGG was added in addition.

583

584 *Flow cytometry*

585 Processing of dLNs and downstream flow cytometric analysis was performed as previously
586 described.³ For both *in vivo* and *in vitro* experiments all incubations were 20 minutes on ice except
587 for Fc block incubations (10 minutes) and antibody staining of fixed and permeabilized cells (45
588 minutes to 1 hour). For human experiments, excess mouse gamma globulin was used to block, as
589 anti-human fluorochrome conjugates were mouse IgG antibodies. See Supplementary Tables 2 and
590 3 for mouse and human flow cytometry reagents, respectively.

591

592 For both mouse and human experiments, we used our previously-established intracellular staining
593 technique⁹ to sensitively and specifically detect IgE-expressing cells. Briefly, to prevent the
594 detection of IgE captured by non-IgE-expressing cells, surface IgE was blocked with a large excess
595 of unconjugated α IgE (clone RME-1 for mouse experiments, clone MHE-18 for human
596 experiments). IgE-expressing cells were then detected after fixation/permeabilization by staining
597 with a low concentration of fluorescently-labelled α IgE of the same clone.

598

599 After staining, cells were collected on an LSRFortessa (BD). Data were analyzed using FlowJo
600 v10. Counting beads were identified by their high SSC and extreme fluorescence and were used
601 to determine the proportion of the cells plated for staining that had been collected on the flow
602 cytometer for each sample. Cells were gated on FSC-W versus FSC-H and then SSC-W versus
603 SSC-H gates to exclude doublets, and next as negative for the fixable viability dye eFluor780 and
604 over a broad range of FSC-A to capture resting and blasting live lymphocytes. 2D plots were
605 presented as contour plots with outliers shown as dots.

606

607 *Phosflow*

608 One million splenocytes in 200 μ L cRPMI/well were plated in a 96-well Microtest U-bottom plates
609 (BD Falcon). Different conditions were plated in duplicate. Wortmannin or an equivalent volume
610 of vehicle control (DMSO) was added to a final concentration of 200nM. Cells were then incubated
611 at 37°C for 10 minutes in a 5% CO₂ incubator to allow inhibitor binding. Cells were pelleted at
612 730 \times g and then resuspended using 25 μ L of either control or α IgD-containing solution, each of
613 which also contained fixable viability dye eFluor780 at a 1/500 dilution. Cells were returned to the
614 incubator for a further 10 minutes to allow for BCR signaling-dependent phosphorylation events
615 and viability staining. After this incubation, 100 μ L of Phosflow Fix Buffer 1 (BD Biosciences),
616 pre-warmed to 37°C, was added to each well and cells were incubated for a further 11 minutes.
617 Cells were pelleted at 930 \times g, washed twice with FACS buffer, then stained for surface markers
618 on ice as normal. Following surface staining, cells were washed then permeabilized with
619 200 μ L/well Phosflow Perm/Wash Buffer 1 (BD Biosciences) for 23 minutes at room temperature.
620 Cells were then pelleted at 930 \times g and resuspended in 25 μ L of Phosflow Perm/Wash Buffer 1
621 containing 1/5-diluted α pS6-AF647 and incubated at room temperature for 1 hour. After staining,
622 cells were washed and resuspended in FACS buffer prior to analysis by flow cytometry.

623

624 *Statistical analysis*

625 To achieve power to discern meaningful differences, experiments were performed with multiple
626 biological replicates and/or multiple times, see figure legends. The number of samples chosen for

627 each comparison was determined based on past similar experiments to gauge the expected
628 magnitude of differences. GraphPad Prism v9 was used for statistical analyses. Data approximated
629 a log-normal distribution and thus were log transformed for statistical tests. Statistical tests were
630 selected by consulting the GraphPad Statistics Guide according to experimental design. All tests
631 were two-tailed. Groups were assumed to have similar standard deviation for ANOVA analysis.

Supplementary Table 1. Šídák's multiple comparisons testing of repeated measures ANOVA

Left side of Figure 4C	Summary	Adjusted P Value
neg vs. neg + α IgD	****	<0.0001
veh vs. veh + α IgD	****	<0.0001
Ibrutinib (50nM) vs. ibrutinib (50nM) + α IgD	****	<0.0001
Ibrutinib (10nM) vs. ibrutinib (10nM) + α IgD	****	<0.0001
Ibrutinib (1nM) vs. ibrutinib (1nM) + α IgD	****	<0.0001
PRT062607 (4uM) vs. PRT062607 (4uM) + α IgD	ns	>0.9999
PRT062607 (2.5uM) vs. PRT062607 (2.5uM) + α IgD	ns	>0.9999
PRT062607 (1uM) vs. PRT062607 (1uM) + α IgD	****	<0.0001
PRT062607 (.4uM) vs. PRT062607 (.4uM) + α IgD	****	<0.0001
Omipalisib (10nM) vs. omipalisib (10nM) + α IgD	****	<0.0001
Omipalisib (5nM) vs. omipalisib (5nM) + α IgD	****	<0.0001
Omipalisib (1nM) vs. omipalisib (1nM) + α IgD	****	<0.0001
Idelalisib (250nM) vs. idelalisib (250nM) + α IgD	****	<0.0001
Idelalisib (5nM) vs. idelalisib (5nM) + α IgD	****	<0.0001
Idelalisib (10nM) vs. idelalisib (10nM) + α IgD	****	<0.0001
neg vs. veh	ns	>0.9999
veh vs. ibrutinib (50nM)	ns	0.9968
veh vs. ibrutinib (10nM)	ns	0.416
veh vs. ibrutinib (1nM)	*	0.0455
veh vs. PRT062607 (4uM)	****	<0.0001
veh vs. PRT062607 (2.5uM)	ns	0.0671
veh vs. PRT062607 (1uM)	ns	0.5302
veh vs. PRT062607 (.4uM)	ns	0.9692
veh vs. omipalisib (10nM)	****	<0.0001
veh vs. omipalisib (5nM)	****	<0.0001
veh vs. omipalisib (1nM)	****	<0.0001
veh vs. idelalisib (250nM)	****	<0.0001
veh vs. idelalisib (5nM)	****	<0.0001
veh vs. idelalisib (10nM)	****	<0.0001
neg + α IgD vs. veh + α IgD	ns	0.9966
neg + α IgD vs. ibrutinib (50nM) + α IgD	****	<0.0001
neg + α IgD vs. ibrutinib (10nM) + α IgD	****	<0.0001
neg + α IgD vs. ibrutinib (1nM) + α IgD	**	0.0023
neg + α IgD vs. PRT062607 (4uM) + α IgD	****	<0.0001
neg + α IgD vs. PRT062607 (2.5uM) + α IgD	****	<0.0001
neg + α IgD vs. PRT062607 (1uM) + α IgD	****	<0.0001
neg + α IgD vs. PRT062607 (.4uM) + α IgD	****	<0.0001
neg + α IgD vs. omipalisib (10nM) + α IgD	****	<0.0001
neg + α IgD vs. omipalisib (5nM) + α IgD	****	<0.0001
neg + α IgD vs. omipalisib (1nM) + α IgD	****	<0.0001
neg + α IgD vs. idelalisib (250nM) + α IgD	****	<0.0001
neg + α IgD vs. idelalisib (5nM) + α IgD	****	<0.0001
neg + α IgD vs. idelalisib (10nM) + α IgD	ns	0.9994

Right side of Figure 4C	Summary	Adjusted P Value
veh vs. veh + α IgD	**	0.0023
Wortmannin (40nM) vs. wortmannin (40nM) + α IgD	**	0.0011
Wortmannin (200nM) vs. wortmannin (200nM) + α IgD	**	0.0052
veh vs. wortmannin (40nM)	ns	0.49
veh vs. wortmannin (200nM)	ns	0.9675
veh + α IgD vs. wortmannin (40nM) + α IgD	ns	0.8761
veh + α IgD vs. wortmannin (200nM) + α IgD	ns	0.1153

Supplementary Table 2: Antibody-fluorochrome conjugates and other reagents used for flow cytometry in mouse experiments

Antibody target or reagent designation	Clone	Company	Conjugate	Dilution
B220	RA3-6B2	BD Biosciences	V500	1/100
		Invitrogen	Qdot 655	1/100-400 (varies by lot)
			APC	1/200
CD38	90	eBioscience	Alexa Fluor 700	1/100
		BD Biosciences	Brilliant Violet 786	1/200
CD45.1	A20	BD Biosciences	Alexa Fluor 647	1/200
			Alexa Fluor 700	1/100
CD45.2	104	BioLegend	Biotin	1/400
			FITC	1/100
			Brilliant Violet 785	1/100
CD138	281-2	BD Biosciences	Brilliant Violet 711	1/175
Fixable Viability Dye eFluor 780	N/A	eBioscience	N/A	1/600-1000
IgD	11-26c.2a	BioLegend	PerCP-Cy5.5	1/200
			Alexa Fluor 700	1/100
IgE	RME-1	BioLegend	Unconjugated	1/15
			FITC	1/300-500
			PE	1/300-500
IgG1	A85-1	BD Biosciences	V450	1/300-400
			FITC	1/300-400
Ig $\lambda_{1,2,3}$	R26-46	BD Biosciences	FITC	1/200
IgM	II/41	eBioscience	PE-Cy7	1/175-1/400
NP	N/A	Conjugated in-house as described. ¹⁰	APC	1/750 of 0.1 mg/mL stock
phosphoS6	N7-548	BD Biosciences	Alexa Fluor 647	1/5
PNA (peanut agglutinin)	N/A	Vector Laboratories	Biotin	1/1000
			FITC	1/500
Streptavidin	N/A	Invitrogen	QDot 605	1/400
		BD Biosciences	Brilliant Violet 711	1/400
TruStain FcX (anti-mouse CD16/32)	93	BioLegend	Unconjugated	1/50

Supplementary Table 3: Antibody-fluorochrome conjugates and other reagents used for flow cytometry in human experiments

Antibody target or reagent designation	Clone	Company	Conjugate	Dilution
CD20	2H7	BioLegend	Pacific Blue	1/200
CD27	O323	BioLegend	PE	1/50
CD38	HB-7	BioLegend	PE-Cy7	1/200
Fixable Viability Dye eFluor 780	N/A	eBioscience	N/A	1/600-1000
IgD	IA6-2	BioLegend	PerCP-Cy5.5	1/50
IgE	MHE-18	BioLegend	Unconjugated	1/10
			APC	1/150-300
IgG1	IS11-12E4.23.30	Miltenyi Biotec	biotin	1/150-300
IgG4	HP6025	SouthernBiotech	FITC	1/800
IgM	MHM-88	BioLegend	Brilliant Violet 605	1/125-1/200
Streptavidin	N/A	Invitrogen	QDot 605	1/400
		BD Biosciences	Brilliant Violet 711	1/400
Mouse gamma globulin	N/A	Jackson ImmunoResearch	Unconjugated	1/100

Acknowledgements

We thank J. Taunton and G.A. Smith for generously providing ibrutinib for our studies. We thank J.G. Cyster, K.M. Ansel, J. Zikherman, and J.F.E. Koenig for advice and comments on the study. This research was supported by the National Institute of Allergy and Infectious Diseases of the National Institutes of Health under Award Numbers R01AI130470 and R21AI154335; the Sandler Asthma Basic Research Center; and the Cardiovascular Research Institute at UCSF. C.D.C. Allen was a Pew Scholar in the Biomedical Sciences, supported by The Pew Charitable Trusts. A.K. Wade-Vallance was supported by a Doctoral Foreign Study Award from the Canadian Institute of Health Research, funding reference number DFD-170769. The content is solely the responsibility of the authors and does not necessarily represent the official views of the funding agencies.

References

1. Wade-Vallance, A. K. & Allen, C. D. C. Intrinsic and extrinsic regulation of IgE B cell responses. *Curr Opin Immunol* **72**, 221–229 (2021).
2. Yang, Z., Wu, C.-A. M., Targ, S. & Allen, C. D. C. IL-21 is a broad negative regulator of IgE class switch recombination in mouse and human B cells. *J Exp Medicine* **217**, e20190472 (2020).
3. Wade-Vallance, A. K. *et al.* B cell receptor ligation induces IgE plasma cell elimination. *J Exp Med* **220**, e20220964 (2023).
4. Omori, S. A. *et al.* Regulation of Class-Switch Recombination and Plasma Cell Differentiation by Phosphatidylinositol 3-Kinase Signaling. *Immunity* **25**, 545–557 (2006).
5. Hauser, J. *et al.* B-cell receptor activation inhibits AID expression through calmodulin inhibition of E-proteins. *P Natl Acad Sci Usa* **105**, 1267–72 (2008).
6. Jabara, H. H. *et al.* B-cell receptor cross-linking delays activation-induced cytidine deaminase induction and inhibits class-switch recombination to IgE. *J Allergy Clin Immun* **121**, 191-196.e2 (2008).
7. Heltemes-Harris, L. M., Gearhart, P. J., Ghosh, P. & Longo, D. L. Activation-induced deaminase-mediated class switch recombination is blocked by anti-IgM signaling in a phosphatidylinositol 3-kinase-dependent fashion. *Mol Immunol* **45**, 1799–1806 (2008).
8. Haniuda, K., Fukao, S., Kodama, T., Hasegawa, H. & Kitamura, D. Autonomous membrane IgE signaling prevents IgE-memory formation. *Nat Immunol* **17**, 1109–1117 (2016).
9. Yang, Z., Sullivan, B. M. & Allen, C. D. C. Fluorescent In Vivo Detection Reveals that IgE+ B Cells Are Restrained by an Intrinsic Cell Fate Predisposition. *Immunity* **36**, 857–872 (2012).
10. Yang, Z. *et al.* Regulation of B cell fate by chronic activity of the IgE B cell receptor. *eLife* **5**, e21238 (2016).
11. Udoe, C. C. *et al.* B-cell receptor physical properties affect relative IgG1 and IgE responses in mouse egg allergy. *Mucosal Immunol* 1–14 (2022) doi:10.1038/s41385-022-00567-y.
12. Baba, Y. & Kurosaki, T. Role of Calcium Signaling in B Cell Biology - Book Chapter - Current topics in Microbiology and Immunology. *Curr Top Microbiol* **393**, 143–174 (2015).
13. Ramadani, F. *et al.* The PI3K Isoforms p110 α and p110 δ Are Essential for PreB Cell Receptor Signaling and B Cell Development. *Sci. Signal.* **3**, ra60 (2010).
14. Clayton, E. *et al.* A Crucial Role for the p110 δ Subunit of Phosphatidylinositol 3-Kinase in B Cell Development and Activation. *J. Exp. Med.* **196**, 753–763 (2002).

15. Okkenhaug, K. *et al.* Impaired B and T Cell Antigen Receptor Signaling in p110 δ PI 3-Kinase Mutant Mice. *Science* **297**, 1031–1034 (2002).
16. Zhang, T. *et al.* Genetic or pharmaceutical blockade of p110 δ phosphoinositide 3-kinase enhances IgE production. *J Allergy Clin Immunol* **122**, 811-819.e2 (2008).
17. Wang, J. *et al.* PTEN-Regulated AID Transcription in Germinal Center B Cells Is Essential for the Class-Switch Recombination and IgG Antibody Responses. *Front Immunol* **9**, 371 (2018).
18. Suzuki, A. *et al.* Critical Roles of Pten in B Cell Homeostasis and Immunoglobulin Class Switch Recombination. *J Exp Medicine* **197**, 657–667 (2003).
19. Chen, Z. *et al.* Imbalanced PTEN and PI3K Signaling Impairs Class Switch Recombination. *J Immunol* **195**, 5461–5471 (2015).
20. Zhang, T., Makondo, K. J. & Marshall, A. J. p110 δ phosphoinositide 3-kinase represses IgE switch by potentiating BCL6 expression. *J Immunol Baltim Md 1950* **188**, 3700–8 (2012).
21. Allen, C. D. C., Okada, T., Tang, H. L. & Cyster, J. G. Imaging of Germinal Center Selection Events During Affinity Maturation. *Science* **315**, 528–531 (2007).
22. Venkitaraman, A. R., Williams, G. T., Dariavach, P. & Neuberger, M. S. The B-cell antigen receptor of the five immunoglobulin classes. *Nature* **352**, 777–781 (1991).
23. Chan, T. D. *et al.* Antigen Affinity Controls Rapid T-Dependent Antibody Production by Driving the Expansion Rather than the Differentiation or Extrafollicular Migration of Early Plasmablasts. *J Immunol* **183**, 3139–3149 (2009).
24. Paus, D. *et al.* Antigen recognition strength regulates the choice between extrafollicular plasma cell and germinal center B cell differentiation. *J Exp Medicine* **203**, 1081–1091 (2006).
25. Sonoda, E. *et al.* B Cell Development under the Condition of Allelic Inclusion. *Immunity* **6**, 225–233 (1997).
26. Reth, M., Hämmerling, G. J. & Rajewsky, K. Analysis of the repertoire of anti-NP antibodies in C57BL/6 mice by cell fusion. I. Characterization of antibody families in the primary and hyperimmune response. *Eur. J. Immunol.* **8**, 393–400 (1978).
27. Hasbold, J., Lyons, A. B., Kehry, M. R. & Hodgkin, P. D. Cell division number regulates IgG1 and IgE switching of B cells following stimulation by CD40 ligand and IL-4. *Eur. J. Immunol.* **28**, 1040–1051 (1998).
28. Tong, P. & Wesemann, D. R. Molecular Mechanisms of IgE Class Switch Recombination. *Curr Top Microbiol* **388**, 21–37 (2015).

29. Rothschild, G. *et al.* Noncoding RNA transcription alters chromosomal topology to promote isotype-specific class switch recombination. *Sci Immunol* **5**, eaay5864 (2020).
30. Ozaki, K. *et al.* A Critical Role for IL-21 in Regulating Immunoglobulin Production. *Science* **298**, 1630–1634 (2002).
31. Sugai, M. *et al.* Essential role of Id2 in negative regulation of IgE class switching. *Nat Immunol* **4**, 25–30 (2003).
32. Kee, B. L., Rivera, R. R. & Murre, C. Id3 inhibits B lymphocyte progenitor growth and survival in response to TGF- β . *Nat Immunol* **2**, 242–247 (2001).
33. Hauser, J., Grundström, C., Kumar, R. & Grundström, T. Regulated localization of an AID complex with E2A, PAX5 and IRF4 at the Igh locus. *Mol Immunol* **80**, 78–90 (2016).
34. Turner, M. L., Corcoran, L. M., Brink, R. & Hodgkin, P. D. High-Affinity B Cell Receptor Ligation by Cognate Antigen Induces Cytokine-Independent Isotype Switching. *J. Immunol.* **184**, 6592–6599 (2010).
35. McIntyre, T. M., Kehry, M. R. & Snapper, C. M. Novel in vitro model for high-rate IgA class switching. *J. Immunol. (Baltim., Md : 1950)* **154**, 3156–61 (1995).
36. Srinivasan, L. *et al.* PI3 Kinase Signals BCR-Dependent Mature B Cell Survival. *Cell* **139**, 573–586 (2009).
37. Reif, K. *et al.* Cutting Edge: Differential Roles for Phosphoinositide 3-Kinases, p110 γ and p110 δ , in Lymphocyte Chemotaxis and Homing. *J. Immunol.* **173**, 2236–2240 (2004).
38. Cutrina-Pons, A., Sa, A. D., Fear, D. J., Gould, H. J. & Ramadani, F. Inhibition of PI3K p110 δ activity reduces IgE production in IL-4 and anti-CD40 stimulated human B cell cultures. *Immunology* **170**, 483–494 (2023).
39. Crotty, S. T Follicular Helper Cell Biology: A Decade of Discovery and Diseases. *Immunity* **50**, 1132–1148 (2019).
40. Robinson, M. J. *et al.* IL-4 Haploinsufficiency Specifically Impairs IgE Responses against Allergens in Mice. *J. Immunol.* **198**, 1815–1822 (2017).
41. Wallace, C. H. *et al.* B lymphocytes confer immune tolerance via cell surface GARP-TGF- β complex. *JCI Insight* **3**, e99863 (2018).
42. Sokol, K. & Milner, J. D. The overlap between allergy and immunodeficiency. *Curr Opin Pediatr* **30**, 848–854 (2018).
43. Wu, C.-A. M. *et al.* Genetic engineering in primary human B cells with CRISPR-Cas9 ribonucleoproteins. *J Immunol Methods* **457**, 33–40 (2018).